

Chapman University  
Chapman University Digital Commons

Pharmacy Faculty Articles and Research

School of Pharmacy

5-23-2014


# Structural Similarity between $\beta$ 3-Peptides Synthesized from $\beta$ 3-Homo-amino Acids or L-Aspartic Acid Monomers

Sahar Ahmed  
*University of Alberta*

Tara Sprules  
*McGill University*

Kamaljit Kaur  
*Chapman University, [kkaur@chapman.edu](mailto:kkaur@chapman.edu)*

Follow this and additional works at: [https://digitalcommons.chapman.edu/pharmacy\\_articles](https://digitalcommons.chapman.edu/pharmacy_articles)

 Part of the [Amino Acids, Peptides, and Proteins Commons](#), [Chemical and Pharmacologic Phenomena Commons](#), [Medical Biochemistry Commons](#), [Medicinal and Pharmaceutical Chemistry Commons](#), and the [Other Pharmacy and Pharmaceutical Sciences Commons](#)

## Recommended Citation

Ahmed S, Sprules T, Kaur K. Structural similarity between  $\beta$ 3-Peptides synthesized from and  $\beta$ 3-homo-amino acids and L-aspartic acid monomers. *Pept Sci*. 2014; 102:359-367. doi: 10.1002/bip.22510

This Article is brought to you for free and open access by the School of Pharmacy at Chapman University Digital Commons. It has been accepted for inclusion in Pharmacy Faculty Articles and Research by an authorized administrator of Chapman University Digital Commons. For more information, please contact [laughtin@chapman.edu](mailto:laughtin@chapman.edu).

---

# Structural Similarity between $\beta$ 3-Peptides Synthesized from $\beta$ 3-Homo-amino Acids or L-Aspartic Acid Monomers

## Comments

This is the accepted version of the following article:

Ahmed S, Sprules T, Kaur K. Structural similarity between  $\beta$ 3-Peptides synthesized from and  $\beta$ 3-homo-amino acids and L-aspartic acid monomers. *Pept Sci.* 2014; 102:359-367.

which has been published in final form at DOI: [10.1002/bip.22510](https://doi.org/10.1002/bip.22510). This article may be used for non-commercial purposes in accordance with [Wiley Terms and Conditions for Self-Archiving](#).

## Copyright

Wiley

# Structural Similarity between $\beta^3$ -Peptides Synthesized from $\beta^3$ -Homo-amino Acids or L- Aspartic Acid Monomers

Sahar Ahmed,<sup>1,2</sup> Tara Sprules,<sup>3</sup> and Kamaljit Kaur<sup>1,\*</sup>

<sup>1</sup>Faculty of Pharmacy and Pharmaceutical Sciences, University of Alberta, Edmonton, Alberta, Canada, T6G 2E1

<sup>2</sup> Department of Pharmacognosy and Medicinal Chemistry, Faculty of Pharmacy, Taibah University, Al-Madinah Al-munawarah 41477, Kingdom of Saudi Arabia

<sup>3</sup>Quebec/Eastern Canada High Field NMR Facility, McGill University, Montreal, Quebec, H3A 2A7

**RECEIVED DATE (to be automatically inserted after your manuscript is accepted if required according to the journal that you are submitting your paper to)**

Tel. 780-492-8917; Fax. 780-492-1217; email. [kkaur@ualberta.ca](mailto:kkaur@ualberta.ca)

Key Words:  $\beta^3$ -peptides, L-aspartic acid monomers, solution conformation, 14-helical structure

## ABSTRACT

Formation of stable secondary structures by oligomers that mimic natural peptides is a key asset for enhanced biological response.  $\beta^3$ -Peptides with an additional methylene group in their backbone are proteolytically stable and fold into stable 14-helical structures in solution. Here we show that oligomeric  $\beta^3$ -hexapeptides synthesized from L-aspartic acid monomers ( $\beta^3$ -peptides **1**, **5a** and **6**) or homologated  $\beta^3$ -amino acids ( $\beta^3$ -peptide **2**), fold into similar stable 14-helical secondary structures in solution, except that the former form right-handed 14-helix and the later form left-handed 14-helix.  $\beta^3$ -Peptides from L-Asp monomers contain an additional amide bond in the side chains that provides opportunities for more hydrogen bonding. However based on the NMR solution structures, we found that  $\beta^3$ -peptide from L-Asp monomers (**1**) and from homologated amino acids (**2**) form similar structures with no additional side chain interactions. These results suggest that the  $\beta^3$ -peptides derived from L-Asp are promising peptide-mimetics that can be readily synthesized using L-Asp monomers as well as the right-handed 14-helical conformation of these  $\beta^3$ -peptides (such as **1** and **6**) may prove beneficial in the design of mimics for right-handed  $\alpha$ -helix of  $\alpha$ -peptides.

## INTRODUCTION

Peptidomimetic molecules play a key role in improving the biological response of  $\alpha$ -peptides by stabilizing their secondary structure and increasing stability toward proteolysis.<sup>1-3</sup> For instance, peptide performance has been improved through partial or total replacement of  $\alpha$ -amino acids with  $\beta$ -amino acids to give  $\alpha/\beta$ -peptide or  $\beta$ -peptides, respectively.<sup>4-13</sup>  $\beta^3$ -amino acids obtained from homologation of  $\alpha$ -amino acids ( $\beta^3$ -homo-amino acids)<sup>14</sup> or from L-Asp monomers ( $\beta^3$ -amido-amino acids, **Scheme 1**)<sup>15,16</sup> are used for the synthesis of  $\beta^3$ -peptides.  $\beta^3$ -amino acids obtained from L-Asp monomers contain an additional amide group in the side chain and therefore are called  $\beta^3$ -amido-amino acids.

$\beta^3$ -Peptides prepared from  $\beta^3$ -homo-amino acids form a characteristic 14-helix secondary structure in solution. Several strategies have been developed to stabilize the 14-helical secondary structure of  $\beta^3$ -peptides, especially in aqueous environments. Some of these strategies include salt bridge or lactam formation between complementary charged  $i/i+3$  side chains, as well as introduction of cyclic residues.<sup>17-21</sup> Formation of stable secondary structure in membrane mimicking solvents such as 2,2,2-trifluoroethanol (TFE) is also important as several peptides act on membrane-bound protein receptors. We previously found that a  $\beta^3$ -hexapeptide (**1**) synthesized from L-Asp monomers formed a stable right handed 14-helix in TFE,<sup>22</sup> and replacement of three  $\alpha$ -amino acids with  $\beta^3$ -amido amino acids in a  $\alpha$ -decapeptide led to the discovery of  $\alpha/\beta$  hybrid peptides that were proteolytically stable and displayed better binding to breast cancer cells compared to the native  $\alpha$ -peptide.<sup>8</sup> Based on these findings and the ease of synthesis,<sup>15</sup> we set out to explore the folding behavior, in particular 14-helix formation, in  $\beta^3$ -peptides derived from L-Asp monomers.

## RESULTS AND DISCUSSION

**Design and synthesis of  $\beta^3$ -peptide 1 analogues.** Seven new analogues of  $\beta^3$ -peptide **1** (Figure 1, 3-6) were designed to study the folding behavior of  $\beta^3$ -peptides derived from L-Asp monomers in TFE and aqueous conditions.  $\beta^3$ -Peptide **1** is a hexapeptide that forms two turns of the 14-helix in TFE, and is unstructured in aqueous conditions.<sup>22</sup>  $\beta^3$ -Peptide **1** analogues ( $\beta^3$ -peptides **3-6**) were designed to study the minimum length required for 14-helical structure and the effect of salt-bridge forming side chains in stabilizing the 14-helical conformation. A  $\beta^3$ -hexapeptide **2** constructed from  $\beta^3$ -homo-amino acids, with the same side chains as  $\beta^3$ -peptide **1**, was included in the study for comparison.

The smallest sequences,  $\beta^3$ -peptides **3a** and **3b**, were four-residues long to incorporate one turn of the 14-helix.  $\beta^3$ -Peptides **4** and **5** were 5-mer and 6-mer, respectively, and each of these contained an amino and a carboxylate side chain at positions  $i$  and  $i+3$  for potential salt bridge formation in the 14-helical conformation. For all the sequences, the side chains with amine groups were either a mimic of Lysine (a analogues) or Ornithine (b analogues). Different lengths of the side chain amine were used to study the effect of side chain length in the formation of ion-pair interaction, as side chain lengths can affect the salt-bridge stability in helical conformations in aqueous environments. Finally,  $\beta^3$ -hexapeptide **6** with two amino side chains and two carboxylate side chains at positions  $i$  and  $i+3$  relative to each other was designed to maximize intramolecular salt-bridge interaction and folding. In all peptides, at least one side of the helix is covered by aliphatic side chains to allow for intramolecular hydrophobic interactions.

$\beta^3$ -Peptides **3-6** were synthesized on the Rink amide MBHA resin essentially following the same procedure as reported for  $\beta^3$ -peptide **1**, whereas  $\beta^3$ -peptide **2** was synthesized by coupling

commercially available Fmoc- $\beta^3$ -homo-amino acids to the Rink amide resin.  $\beta^3$ -Peptides **3-6** were synthesized using orthogonally protected Fmoc-L-Asp monomers or pre-synthesized Fmoc- $\beta^3$ -amido-amino acids.

The general structure of Fmoc- $\beta^3$ -amido-amino acids is shown in **Scheme 1**. Monomeric Fmoc- $\beta^3$ -amido-amino acids, such as Fmoc- $\beta^3$ amV-OH and Fmoc- $\beta^3$ amL-OH (Figure **S1**, supporting information), were prepared using either solid phase or solution phase synthesis as shown in **Scheme 1**. Fmoc- $\beta^3$ amK(Boc)-OH and Fmoc- $\beta^3$ amE(tBu)-OH were prepared using solid phase synthesis method only and were obtained in 50-52% yields. The solution phase method gave much higher yields (80%) compared to the solid phase method (50-64%). All  $\beta^3$ -amino acids were characterized by NMR and mass spectrometry, and the purity was assessed by analytical HPLC (**Figure S1**).

Shorter sequences, **3** and **4**, were synthesized by coupling orthogonally protected Fmoc-L-Asp where the side chain was introduced during the SPPS, while the synthesis of hexapeptides **5** and **6**, utilized pre-synthesized monomeric Fmoc- $\beta^3$ -amido-amino acids. The completed peptide sequences were cleaved from the resin followed by purification using RP-HPLC prior to characterization by NMR spectroscopy, mass spectrometry and analytical HPLC (**Tables S1-S9** and **Figure S2**). All peptides were obtained in good yields (>50%).

Protected  $\beta^3$ -amino acids building blocks (from L-Asp) were prepared to determine if the overall yield of long  $\beta^3$ -peptides can be increased. Peptides **5** and **6** were obtained in relatively high yields (81-90%) due to the use of  $\beta^3$ -amido amino acid monomers (or protected  $\beta^3$ -amino acids building blocks) instead of orthogonally protected L-Asp.

**Circular dichroism spectroscopy of  $\beta^3$ -peptides in TFE and aqueous conditions.** The solution conformation of  $\beta^3$ -peptides was evaluated in TFE and water using CD spectroscopy. The CD spectra provide an initial estimate of solution conformation in a relatively short time based on the intensity of a negative minimum at 214 nm. A minimum at 214 nm for  $\beta^3$ -peptides is considered as a signature for 14-helical conformation and the intensity of the peak is correlated with the 14-helical content.

First we compared the 14-helical folding of the five hexapeptides in TFE, a helix-stabilizing solvent.<sup>23,24</sup> As shown in **Figure 2a**, the mean residue ellipticity (MRE) values at 214 nm were significantly different for the five  $\beta^3$ -peptides. Surprisingly, **1** shows the largest minima at 214 nm ( $\theta = -20 \times 10^3$ ) suggesting highest helical structure followed by  $\beta^3$ -peptide **6** with the next largest minimum ( $\theta = -16 \times 10^3$ ). The intensity of peaks for hexamers **5a** and **5b** was on the lower side with **5a** (lysine side chain) showing better 14-helicity compared to **5b** (ornithine side chain) suggesting that the length of the side chain forming salt-bridge does have an effect on folding, and the salt bridge between Lys and Glu is more stable than that between Orn and Glu. This trend is similar to what was observed by Luc Brunsveld and coworkers in a systematic study of side-chain to side-chain interacting  $\beta^3$ -peptides. The authors found that in general longer side chain lengths ( $\beta^3$ -homoLys vs.  $\beta^3$ -homoOrn and  $\beta^3$ -homoGlu vs.  $\beta^3$ -homoAsp) displayed slightly better salt bridge stabilization and 14-helix formation.<sup>20</sup> In a previous survey on the preferred partner for intra- $\alpha$ -helical salt bridges in proteins of known structure, it was found to that Glutamate not aspartate was the preferred partner suggesting that longer side chain lengths lead to better ion-pair interaction and folded structure.<sup>25</sup>



$\beta^3$ -Peptide **2** also displays a minimum at 214 nm suggesting 14-helix conformation. The MRE values of  $\beta^3$ -peptide **2** and other hexamers may not be directly comparable as these have very different side chains. Moreover, it is interesting to note that even though the absolute configuration at  $\beta^3$  carbon in  $\beta^3$ -peptides derived from homo-amino acids and L-Asp is opposite, both  $\beta^3$ -peptides (for instance **1** and **2**) have the same sign in the minimum at 214 nm attributed to 14-helix in the CD spectra. Most likely this is due to the major contribution from side chain amides in  $\beta^3$ -peptides prepared from L-Asp monomers. These peptides can be viewed as  $\alpha$ -peptides with substituted L-asparagine residues. Interestingly, Mathews et al<sup>26</sup> observed that the CD spectrum of a fully protected  $\beta^3$ -hexapeptide, (Boc- $[\beta$ -Asp(OBn)- $\beta^3$ -HGlu(Obn)- $\beta^3$ -HSer(OBn)]<sub>2</sub>-OTCE, made from L-Asp, homo-Glu, and homo-Ser residues showed an intense maximum at 198 nm, and two shoulders (maxima) at 207 and 216 nm suggesting opposite handed helical structure compared to  $\beta^3$ -hexapeptides **1**, **5** and **6**.

Next we compared the 14-helix stability of the two hexamers, ( $\beta^3$ -peptide **5a** and **6**) that engage in intramolecular salt-bridge interaction, with decreasing TFE concentration (**Figures 2b and 2c**). For both the peptides, a decrease in the minimum at 214 nm was observed with increase in water concentration suggesting a loss of helical conformation.  $\beta^3$ -Peptide **5a** always maintained 14-helical conformation (20-100% TFE), except in 100% water. A minimum at 214 nm was observed even in 20% TFE ( $\theta = -5 \times 10^3$ ) and the peak was lost only in water.  $\beta^3$ -Peptide **6** displayed similar behavior to that of **5a** in TFE/water mixtures (**Figure 2c**). The CD spectra of  $\beta^3$ -peptide **6** in 100% and 50% TFE show characteristic minima at 214 nm with MRE values  $-16 \times 10^3$  and  $-12 \times 10^3$ , respectively. There is about 25% reduction in the helical content in 50% TFE/water compared to 100% TFE. The spectra show very small peaks in PBC buffer (pH 7.4, 1

mM) and only a small shoulder in water suggesting a dramatic decrease in the helical content. The CD spectrum for **6** was performed in PBS buffer at pH 7.4 to ensure that all amine side chains are protonated and the carboxylate are deprotonated to enhance salt bridge interactions. However, the peptide was definitely less folded in aqueous conditions despite the presence of two ion-pair interactions. The loss of secondary structure in water could be due to the placement of the charged amino acids opposite to the macrodipole. Macrodipole present in  $\beta^3$ -peptides stabilizes secondary structures<sup>19,27,28</sup> and can be maintained by placing basic amino acids such as Lysine and Ornithine near the N-terminus and acidic residues such as Aspartic and Glutamic acid near the C-terminus.<sup>19,20</sup> Nevertheless,  $\beta^3$ -peptide **6** forms a stable 14-helix in TFE. The CD spectra of  $\beta^3$ -peptide **6** at two different concentrations, 200  $\mu$ M and 1 mM, showed similar minima at 214 nm and were found to be independent of concentration suggesting that no changes in aggregation state occur in this concentration range. Finally, the CD spectra of 4-mer and 5-mer  $\beta^3$ -peptides (**3** and **4**) suggested less folded structures compared to the hexamers (**Figure S3**), and did not show a clear signature of 14-helical content. For such short oligomers, NMR spectroscopy would be required for further evaluation of the folded conformation.

**NMR solution structure studies of  $\beta^3$ -peptides.** To probe the secondary structure of  $\beta^3$ -peptides **1** (previously studied), and **2-6** (**Figure 1**) in solution, a detailed NMR spectroscopic investigation was carried out. 1D NMR of all the eight peptides (**2-6**) in TFE- $d_2$  ( $CF_3CD_2OH$ ) was examined, and the presence of a regular secondary structure was indicated by a large dispersion of the chemical shifts. The well dispersed chemical shifts in the amide region allowed assignment of all the backbone and side chain protons (see supporting information, **Tables S2-S9**). A two-

dimensional (2D) NOESY experiment was performed for all the peptides, which allowed observation of NOEs between protons from residues that are not sequentially adjacent. Characteristic 14-helical peaks were observed mainly for  $\beta^3$ -peptides **1**, **2** and **6**. The NOESY spectrum of  $\beta^3$ -hexapeptide **2** showed multiple (five out of six possible) long range  $H\alpha_i \rightarrow H\beta_{i+3}$  (**Figure S4a**). Whereas for  $\beta^3$ -peptide **6**, all possible (six) long range  $H\alpha_i \rightarrow H\beta_{i+3}$  NOEs were observed (**Figure S4b**) suggesting helical conformation in these peptides. Interestingly, the characteristic  $H\alpha_1 \rightarrow H\beta_4$  peaks were also observed for the smallest 4-mer  $\beta^3$ -peptide **3a** suggesting helical conformation (**Figure S4b**). These peaks are a hallmark of 14-helical secondary structure.

The extent of helical folding in different  $\beta$ -peptides can be compared using NOE data. At least four NOE patterns involving backbone and side chain protons that are suggestive of a 14-helix can be compared. These NOE patterns are  $NH_i \rightarrow H\beta_{i+3}$ ,  $NH_i \rightarrow H\beta_{i+2}$ ,  $H\alpha_i \rightarrow H\beta_{i+3}$ , and the sidechain  $CH_{2-i} \rightarrow$  sidechain  $NH_{i+3}$  (or  $H\alpha_i \rightarrow HS_{i+3}$ ). As shown in **Figure 3**, direct comparison of these NOEs showed that  $\beta^3$ -peptides **1**, **2**, and **6** have comparable helical conformation in solution (TFE). Despite the presence of two pairs of oppositely charged side chains in  $\beta^3$ -peptide **6**, the NOEs between the side chain protons of the Glu1-Lys4 and Glu2-Lys5 pairs were relatively weak, suggesting that adoption of a stable conformation is not driven by formation of salt-bridges. The backbone NOEs, such as for  $H\alpha_{11} \rightarrow H\beta_4$  and  $H\alpha_{12} \rightarrow H\beta_4$ , were much stronger. Peptide **5a**, with a single pair of oppositely charged side chains, seems to be the least structured out of the four hexapeptides as it showed only two of the  $H\alpha_i \rightarrow H\beta_{i+3}$  NOEs.

These peptides behaved differently in aqueous conditions. 2D NOESY and TOCSY spectra were recorded for  $\beta^3$ -peptide **6** in 25 mM phosphate buffer at pH 6.1 and 6.6. There was little chemical shift dispersion, therefore hall mark long-range NOEs for 14-helices could not be

identified. This lack of dispersion suggests that the peptide is not (stably) folded. All the backbone amides, H $\alpha$  and H $\beta$  peaks were overlapped. The  $\beta$ -Leu and  $\beta$ -Lys side chain shifts were exactly overlapped. The  $\beta$ -Glu side chain protons had slightly different shifts. This may be due to the fact that one of the  $\beta$ -Glus is the N-terminal residue. These observations agreed with the CD data as the characteristic minima for 14-helix was not observed for the peptides in aqueous conditions. The NMR data suggests that the peptides were not aggregated in water as line widths were comparable to those observed in the spectra recorded in TFE.

The three-dimensional structures of **1** (done previously), **2** and **6** were obtained using the NOE data and the program CYANA.<sup>29</sup> The input data and structure calculation statistics of peptides **2** and **6** are summarized in **Tables S10** and **S11**. The pdb coordinates of the 20 structures obtained from CYANA program were averaged to obtain the final peptide structures in TFE (**Figure 4**).  $\beta^3$ -hexapeptides **1** and **6** form a right-handed 14-helical structure with a radius of 2.6 Å and 4.69 Å rise/turn. In contrast, the  $\beta^3$ -hexapeptide **2** made up of  $\beta$ homo-amino acids, forms a left-handed 14-helix (**Figures 5** and **S5**). The difference in the conformation of the two helices (right-handed versus left-handed) could be due to the opposite stereochemistry at the  $\beta^3$  carbon in the peptide backbone. The radius and the pitch for the two helices are found to be similar.

The extra amide bond in the side chain of  $\beta^3$ -peptides derived from L-Asp monomers provides opportunities for additional hydrogen bonding capabilities and perhaps unprecedented secondary structures. However, we found that the side chain amide bonds in these  $\beta^3$ -peptides (**1**, **5a**, and **6**) do not seem to interact much except that for  $\beta^3$ -peptide **1** we see a  $\beta$ Leu3 side chain O to  $\beta$ Leu6 side chain N hydrogen bond possible in some structures. All possible NOEs were incorporated into the structure calculations, and clearly there were not enough contacts observed

between the  $i$  and  $i+3$  side chains to constrain them in a way to give consistent hydrogen bonds in the side chains.

## CONCLUSIONS

In summary, we show that  $\beta^3$ -peptides can readily be synthesized from L-Asp monomers and for the first time compare the solution conformation of  $\beta^3$ -peptides synthesized from  $\beta^3$ -homoamino acids and L-Asp monomers. Both  $\beta^3$ -peptides form similar 14-helix structure which can be stabilized by salt-bridge interactions of the side chains at  $i$  and  $i+3$  positions in conjunction with a maintained helix macrodipole. The  $\beta^3$ -hexapeptides reported here with the charged side chains (**5** and **6**) at  $i$  and  $i+3$  positions, however, did not have the basic and acidic side chains in the correct order to stabilize the helix macrodipole and therefore, did not give stable structures compared to the  $\beta^3$ -peptide with no salt-bridge interaction ( $\beta^3$ -peptide **1**). The synthesis of  $\beta^3$ -peptides with charged residues that will maintain the helix macrodipole is currently in progress. The findings presented here show that  $\beta^3$ -peptides derived from L-Asp will facilitate the design and development of peptidomimetics with improved biological properties.

## MATERIALS AND METHODS

**Solvents and reagents.** Rink amide methylbenzhydrylamine (MBHA) resin (0.58 mmol/g), 2-chlorotrityl chloride resin (1.4 mmol/g), N- $\alpha$ -Fmoc-L-aspartic acid  $\alpha$ -allyl ester, Fmoc-Asp(OtBu)-OH, Boc-L-asparagine, Fmoc- $\beta^3$ hLeu-OH, Fmoc- $\beta^3$ hLys(Boc)-OH, Fmoc- $\beta^3$ hVal-OH, tert-butyl N-(4-aminobutyl)carbamate,  $\beta$ -alanine t-butyl ester hydrochloride, 1-hydroxybenzotriazole (HOBt), and benzotriazol-1-yl-oxy-tris-(dimethylamino)-phosphonium hexafluorophosphate

(BOP) were purchased from NovaBiochem (San Diego, CA). Isobutylamine, isopropylamine, dimethylformamide (DMF), N-methyl morpholine (NMM), trifluoroacetic acid (TFA), and all other reagents were purchased from Sigma-Aldrich (St Louis, MO, USA). Piperidine was purchased from Caledon. All commercial reagents and solvents were used as received. Silica gel for column chromatography was obtained from Rose Scientific Ltd. Column chromatography was performed under slight positive air pressure using silica gel 60 (70-230 mesh).

**Equipment.** RP-HPLC purification and analysis were carried out on a Waters (625 LC system) HPLC system using auto-injector mode or Varian Prostar HPLC system (Walkersville, MD, USA) using manual injector. Vydac C18 semi-preparative (1 x 25 cm, 5  $\mu$ m) and analytical (0.46 x 25 cm, 5  $\mu$ m) columns were used. Peptides were detected by UV absorption at 220 nm. Mass spectra were recorded on a matrix-assisted laser desorption ionization time-of-flight (MALDI-TOF) Voyager spectrometer (Voyager<sup>TM</sup> Elite) or Waters micromass ZQ (Waters Corp., Milford, MA, USA) mass spectrometer. CD measurements were made on an olis CD spectrometer (Georgia, USA) at 25 °C in a thermally controlled quartz cell (Hellma, Plainview, NY). NMR experiments were recorded on a Bruker AM-300 spectrometer at the Faculty of Pharmacy and Pharmaceutical Sciences (University of Alberta), or on a Varian INOVA 500 MHz NMR spectrometer equipped with a triple-resonance HCN Cold Probe with z-axis pulsed field gradients at the Quebec/Eastern Canada High Field NMR Centre, McGill University, Montreal, Quebec. pH measurements for all buffer solutions were done at 25 °C with a digital SB20 Symphony VWR pH meter using a calibration buffer set (Fluka).

**Peptide Synthesis.** The synthesis of  $\beta^3$ -peptide **1** has been reported previously<sup>15</sup> and eight  $\beta^3$ -peptides (**2-6**) were synthesized following the manual Fmoc-solid phase peptide synthesis. The crude peptides were cleaved from the resin by treatment with TFA:TIPS:H<sub>2</sub>O (96:2:2) cocktail mixture with stirring for 2 h. The crude peptides were purified using semi-preparative RP-HPLC prior to characterization by electrospray and/or MALDI-TOF mass spectrometry and analytical HPLC (**Table S1** and **Figure S2**). All eight peptides were also characterized by 1D proton NMR (**Tables S2-S9**).

$\beta^3$ -Peptide **2** was synthesized by coupling Fmoc- $\beta^3$ h-amino acids (Fmoc- $\beta^3$ hLeu-OH, Fmoc- $\beta^3$ hLys(Boc)-OH or Fmoc- $\beta^3$ hVal-OH) sequentially to the Rink amide MBHA resin using BOP and HOBT as coupling reagents. The syntheses of  $\beta^3$ -peptides **3** and **4** followed the same procedure as reported for  $\beta^3$ -peptide **1** using orthogonally protected Fmoc-L-aspartic acid.<sup>15</sup> Briefly, orthogonally protected L-aspartic acid (*N* <sup>$\alpha$</sup> -Fmoc-L-aspartic acid  $\alpha$ -allyl ester) is coupled to the Rink amide MBHA resin using BOP with HOBT. The side chain allyl group is first removed with Pd(PPh<sub>3</sub>)<sub>4</sub> followed by coupling with an amine (for the corresponding side chain). Next the Fmoc group is removed and orthogonally protected L-aspartic acid is coupled to follow the next cycle till the sequence is complete.

The synthesis of  $\beta^3$ -peptide **5** was accomplished by coupling monomeric Fmoc- $\beta^3$ -amido-amino acid (*N* <sup>$\beta$</sup> -Fmoc- $\beta^3$ amV-OH) to  $\beta^3$ -peptide **4**. For  $\beta^3$ -peptide **6**, orthogonally protected L-aspartic acid was coupled to introduce the first two amino acids, and the last four residues were coupled as monomeric Fmoc- $\beta^3$ -amido-amino acids to complete the sequence. Monomeric Fmoc- $\beta^3$ -amido-amino acids (Fmoc- $\beta^3$ amV-OH, Fmoc- $\beta^3$ amL-OH, Fmoc- $\beta^3$ amK(Boc)-OH, and Fmoc-

$\beta^3$ amE(tBu)-OH) were synthesized using solid phase or solution phase synthesis as described below.

**Solid Phase Synthesis of Fmoc- $\beta^3$ -Amido-Amino Acid Monomers.** Orthogonally protected  $\beta^3$ -amido amino acid monomers were synthesized in four steps as shown in **Scheme 1**. In a solid phase reactor, chlorotrityl resin (74 mg, 0.1 mmol) was suspended in  $\text{CH}_2\text{Cl}_2$  (4 mL) for swelling for 30 min. The swelled resin was reacted with a solution of Fmoc-L-aspartic acid  $\alpha$ -allyl ester (118.6 mg, 3 equiv) and DIPEA (210  $\mu\text{L}$ , 12 equiv) in dry  $\text{CH}_2\text{Cl}_2$  for 2 h. The resin was capped by washing with a solution of dry  $\text{CH}_2\text{Cl}_2$ -MeOH-DIPEA (17:2:1). The resin was washed with DMF (4 x 1 min), DCM (4 x 1 min) and IPA. Deallylation was carried out in the presence of  $\text{Pd}(\text{PPh}_3)_4$  (0.08 equiv) and  $\text{PhSiH}_3$  (8 equiv) in DCM (3 x 35 mins) under nitrogen to remove the side chain allyl protection. Subsequently, the side chain amine (2.5 equiv) was coupled using BOP (110 mg, 2.45 equiv), HOBt (33 mg, 2.5 equiv), and NMM (75  $\mu\text{L}$ , 4.5 equiv) in DMF for 5 h. Cleavage of the monomer from the resin was done either by treating with 50% TFA/DCM for 30 min, or with TFE/DCM (20/80%) for 45 min at room temperature.

**Synthesis of  $\text{N}^\beta$ -Fmoc- $\beta^3$ amV.**  $\text{N}^\beta$ -Fmoc- $\beta^3$ amV-OH was synthesized using the procedure described above. Isopropylamine was coupled after removal of side chain allyl group and the final product was cleaved from the resin using 50% TFA/DCM for 30 min. The residue was added to cold  $\text{Et}_2\text{O}$  (40 mL,  $-78^\circ\text{C}$ ) and centrifuged at 3,500 rpm for 5 min. The  $\text{Et}_2\text{O}$  was decanted and the pellet was resuspended in cold  $\text{Et}_2\text{O}$  (40 mL,  $-78^\circ\text{C}$ ) and centrifugation was repeated three times. Again the  $\text{Et}_2\text{O}$  was decanted and the pellet was dried with  $\text{N}_2$  with an overall yield 65%. The purity was assessed by analytical HPLC as shown in **Figure S1**.  $^1\text{H}$  NMR (300 MHz,  $\text{CD}_3\text{OD}$ ):  $\delta$ = 1.06



(d, J= 6.7, 6H, (CH<sub>3</sub>)<sub>2</sub>CH), 2.6 (m, 2H, CH<sub>2</sub>COOH), 3.94 (m, 1H, (CH<sub>3</sub>)<sub>2</sub> CH), 4.25 (m, 1H, CHCH<sub>2</sub>O), 4.7 (m, 2H, CHCH<sub>2</sub>O), 4.6 (t, 1H, CHCH<sub>2</sub>COOH), 7.2-7.8 (m, 8H, aryl H). <sup>13</sup>C NMR (300 MHz, DMSO-d<sub>6</sub>, CD<sub>3</sub>OD): δ= 19.93, 40.67, 40.76, 46.51, 50.68, 65.50, 119.76, 124.99, 126.80, 127.35, 140.52, 143.57, 155.56, 168.8, 172.87, and ES-MS: Calcd. for C<sub>22</sub>H<sub>24</sub>N<sub>2</sub>O<sub>5</sub>, [M+H]<sup>+</sup> 397.47; found [M+H]<sup>+</sup> 397.06.

**Synthesis of N<sup>β</sup>-Fmoc-β<sup>3</sup>amL.** The synthesis of N<sup>β</sup>-Fmoc-β<sup>3</sup>amL-OH followed the same procedure as for N<sup>β</sup>-Fmoc-β<sup>3</sup>amV-OH, except that isobutylamine was coupled after removal of side chain allyl group with an overall yield of 63%. The purity was assessed by analytical HPLC as shown in **Figure S1**. <sup>1</sup>H NMR (300 MHz, CDCl<sub>3</sub>): δ= 0.96 (d, J=6.6, 6H, (CH<sub>3</sub>)<sub>2</sub>CH), 1.85 (m, 1H, (CH<sub>3</sub>)<sub>2</sub> CH), 2.8 (m, 1H, CH<sub>2</sub>COOH), 2.9 (m, 1H, CH<sub>2</sub>COOH), 3.2 (m, 2H, (CH<sub>3</sub>)<sub>2</sub> CH)CH<sub>2</sub>NH), 4.2 (m, 1H, CHCH<sub>2</sub>O), 4.45 (m, 2H, CHCH<sub>2</sub>O, CHCH<sub>2</sub>COOH), 7.2-7.8 (m, 8H, arylH). <sup>13</sup>C NMR (300 MHz, CDCl<sub>3</sub>): δ= 19.93, 27.9, 36.9, 46.06, 46.51, 50.68, 65.60, 119.76, 124.99, 126.8, 127.35, 140.52, 143.57, 155.56, 168.87, 172.8, and ES-MS: Calcd. for C<sub>23</sub>H<sub>26</sub>N<sub>2</sub>O<sub>5</sub>, [M+H]<sup>+</sup> 411.47; found [M+H]<sup>+</sup> 411.00.

**Synthesis of N<sup>β</sup>-Fmoc-β<sup>3</sup>amK(Boc)-OH.** N<sup>β</sup>-Fmoc-β<sup>3</sup>amK (Boc)-OH was synthesized using the same procedure as described above. The side chain mimicking lysine was introduced by coupling with tert-butyl N-(4-aminobutyl)carbamate after allyl group removal. N<sup>β</sup>-Fmoc-β<sup>3</sup>amK (Boc)-OH was cleaved from the resin using TFE/DCM (2:8) for 45 min to obtain the monomer with an overall of yield 52%. The purity was assessed by analytical HPLC as shown in **Figure S1**. <sup>1</sup>H NMR (300 MHz, CDCl<sub>3</sub>): δ=1.3 (m, 13H, (CH<sub>3</sub>)<sub>3</sub> CH (CH<sub>2</sub>)<sub>2</sub>), 2.2-2.4 (m, 2H, CH<sub>2</sub>COOH), 2.7- 3.1 (m, 4H, (NH)CH<sub>2</sub> CH<sub>2</sub> CH<sub>2</sub> CH<sub>2</sub>NH), 3.7 (m, 4H, CHCH<sub>2</sub>O, 2H, CHCH<sub>2</sub>O, CHCH<sub>2</sub>COOH), 7.2-7.8 (m,

8H, aryl H).  $^{13}\text{C}$  NMR (300 MHz,  $\text{CD}_3\text{OD}$ ):  $\delta$  = 26.34, 26.83, 28.26, 40.69, 40.98, 51.04, 77.30, 119.98, 121.10, 122.17, 123.88, 127.68, 128.88, 129.43, 135.33, 137.36, 139.34, 142.50, 155.52, 170.93, and ES-MS: Calcd.  $\text{C}_{28}\text{H}_{35}\text{N}_3\text{O}_7$ ,  $[\text{M}-\text{H}]^-$  524.25; found  $[\text{M}-\text{H}]^-$  524.

**Synthesis of  $\text{N}^\beta$ -Fmoc- $\beta^3$ amE(tBu)-OH:**  $\text{N}^\beta$ -Fmoc- $\beta^3$ amE(tBu)-OH (**10**) was synthesized using the same procedure as described above for  $\text{N}^\beta$ -Fmoc- $\beta^3$ amK (Boc)-OH. The side chain mimicking glutamic acid was introduced by coupling with  $\beta$ -alanine t-butyl ester hydrochloride after allyl group removal. The overall yield was found to be 50%, and the purity was assessed by analytical HPLC as shown in **Figure S1**.  $^1\text{H}$  NMR (300 MHz, d-DMSO):  $\delta$ = 1.4 (s, 9H,  $(\text{CH}_3)_3\text{C}$ ), 2.5-2.8 (m, 4H,  $\text{CH}_2\text{COOH}$ ,  $\text{CH}_2\text{CH}_2\text{NHCO}$ ), 3.6 (m, 2H,  $\text{CH}_2\text{CH}_2\text{NHCO}$ ), 4.25-4.4 (m, 4H,  $\text{CHCH}_2\text{O}$ ,  $\text{CHCH}_2\text{O}$ ,  $\text{CHCH}_2\text{COOH}$ ), 7.3-7.8 (m, 8H, aryl H).  $^{13}\text{C}$  NMR (300 MHz, d-DMSO):  $\delta$ =27, 34.88, 34.98, 40.34, 46.64, 50.53, 65.77, 79.99, 120.14, 125.28, 127.13, 127.42, 127.68, 140.7, 143.80, 155.82, 170.76, 171.69, 173.04, and ES-MS: Calcd. for  $\text{C}_{26}\text{H}_{30}\text{N}_2\text{O}_7$ ,  $[\text{M}-\text{H}]^-$  481.54; found  $[\text{M}-\text{H}]^-$  481.20.

**Solution Phase Synthesis of Fmoc- $\beta^3$ -Amido-Amino Acid Monomers.**  $\beta^3$ -am-Val and  $\beta^3$ -am-Leu monomers were also synthesized using solution phase synthesis as illustrated in **Scheme 1**. Fmoc-Asp(OtBu)-OH (412 mg, 1 mmol), BOP (442 mg, 1.95 equiv), HOBt (135 mg, 2 equiv) and NMM (200  $\mu\text{L}$ , 4.5 equiv) were weighted into a round bottom flask, and dissolved in DMF/DCM (4 mL). The mixture was stirred for 5 min to activate the carboxyl group, following which the amine side chain (isopropylamine or isobutylamine, 5 equiv) was added and the reaction mixture was stirred for 24 h at room temperature. The completion of reaction was monitored using TLC. The reaction mixture was evaporated to give oil as the residue. The residue was dissolved

in EtOAc (10 mL). The EtOAc was washed with 5% NaHCO<sub>3</sub> three times followed by washing (3x) with brine (0.9% NaCl solution). The organic layer was then dried (Na<sub>2</sub>SO<sub>4</sub>), filtered, and concentrated. The product was characterized using mass spectrometry. After confirmation of the mass, the precipitate was treated with TFA:TIPS:H<sub>2</sub>O (96:2:2) cocktail mixture with stirring for 2 h. The reaction mixture was then evaporated under vacuum and the product was washed several times with diethyl ether. The precipitate obtained was further characterized with mass spectrometry, HPLC, and NMR spectroscopy. The overall yield was 80.5%. The product was used without further purification.

**Circular Dichroism.** All CD measurements were made on an Olis CD spectrometer (Georgia, USA) at 25 °C in 2 mm path length thermally controlled quartz cell, over 190-260 nm. All samples were prepared in the appropriate solvents immediately prior to recording the spectra (TFE, H<sub>2</sub>O, or PBS). Spectra represent the average of five scans, and were background-corrected and smoothed. Each peptide was analyzed at concentrations of 100, 200, 250, and 500 μM. Peptide concentrations were determined using dry weight of the lyophilized peptide. Spectra were normalized to mean residue ellipticity (deg cm<sup>2</sup> dmol<sup>-1</sup>) using the formula  $A * M * 3298 / (L * C)$ , where C is concentration in g/L, M is average molecular weight (g/mol), L is path length of the cell.<sup>30</sup>

**Two-dimensional NMR and Structure Elucidation of β<sup>3</sup>-Peptides 2 and 6.** All 2D NMR measurements and structure elucidation was done at Quebec/Eastern Canada High Field NMR Centre, McGill University, Montreal, Quebec. A 1.5 mM sample of peptides **2** or **6** in 100% TFE-d<sub>2</sub> (CF<sub>3</sub>CD<sub>2</sub>OH) (Cambridge Isotope Laboratories, Inc.) was prepared for 2D NMR experiments.

Sequence specific assignments were established by following the procedures used for  $\alpha$ -amino acid peptides.<sup>31</sup> 2D TOCSY (60 ms mixing time), COSY and NOESY (mixing time 300 ms) spectra were recorded at 10 °C on a Varian INOVA 500 MHz spectrometer. The upper distance restraints for **2** and **6** were obtained from a 300 ms mixing time 2D-NOESY recorded at 10 °C on a Varian INOVA 800 MHz NMR spectrometer, equipped with an HCN cold probe and pulsed-field gradients. Calculation of the complete three-dimensional structure was performed with the program CYANA v2.<sup>29</sup> The structure calculation statistics for **2** and **6** are summarized in **Tables S10** and **S11**, respectively. The final calculations were started with 200 randomized conformers all of which converged to the helical conformation (average backbone RMSD to mean for 200 structures:  $0.54 \pm 0.10$  Å for  $\beta^3$ -peptide **2** and  $0.50 \pm 0.12$  Å for  $\beta^3$ -peptide **6**). A bundle of the 20 lowest energy CYANA conformers were used to represent the NMR structures of **2** and **6** (**Figure 4**).

## SUPPORTING INFORMATION

Peptide characterization and data for three-dimensional NMR solution structures of **2** and **6**.

## ACKNOWLEDGEMENTS

This work was supported by the Natural Sciences and Engineering Research Council of Canada (NSERC).

## References

- (1) Cheng, R. P.; Gellman, S. H.; DeGrado, W. F. *Chemical Reviews* 2001, 101, 3219-3232.

- (2) Goodman, C. M.; Choi, S.; Shandler, S.; DeGrado, W. F. *Nature Chemical Biology* 2007, 3, 252-262.
- (3) Seebach, D.; Beck, A. K.; Bierbaum, D. J. *Chemistry & Biodiversity* 2004, 1, 1111-1239.
- (4) Denton, E. V.; Craig, C. J.; Pongratz, R. L.; Appelbaum, J. S.; Doerner, A. E.; Narayanan, A.; Shulman, G. I.; Cline, G. W.; Schepartz, A. *Org Lett* 2013, 15, 5318-5321.
- (5) English, E. P.; Chumanov, R. S.; Gellman, S. H.; Compton, T. J. *J Biol Chem* 2006, 281, 2661-2667.
- (6) Horne, W. S.; Johnson, L. M.; Ketas, T. J.; Klasse, P. J.; Lu, M.; Moore, J. P.; Gellman, S. H. *Proc Natl Acad Sci U S A* 2009, 106, 14751-14756.
- (7) Kritzer, J. A.; Zutshi, R.; Cheah, M.; Ran, F. A.; Webman, R.; Wongjirad, T. M.; Schepartz, A. *Chembiochem* 2006, 7, 29-31.
- (8) Soudy, R.; Gill, A.; Sprules, T.; Lavasanifar, A.; Kaur, K. *J Med Chem* 2011, 54, 7523-7534.
- (9) Kritzer, J. A.; Lear, J. D.; Hodsdon, M. E.; Schepartz, A. *J Am Chem Soc* 2004, 126, 9468-9469.
- (10) Raguse, T. L.; Porter, E. A.; Weisblum, B.; Gellman, S. H. *J Am Chem Soc* 2002, 124, 12774-12785.
- (11) Kolesinska, B.; Podwysocka, D. J.; Rueping, M. A.; Seebach, D.; Kamena, F.; Walde, P.; Sauer, M.; Windschiegl, B.; Meyer-Acs, M.; Bruggen, M. V. D.; Giehring, S. *Chemistry & Biodiversity* 2013, 10, 1-38.
- (12) Lee, E. F.; Smith, B. J.; Horne, W. S.; Mayer, K. N.; Evangelista, M.; Colman, P. M.; Gellman, S. H.; Fairlie, W. D. *Chembiochem* 2011, 12, 2025-2032.

- (13) Smith, B. J.; Lee, E. F.; Checco, J. W.; Evangelista, M.; Gellman, S. H.; Fairlie, W. D. *Chembiochem* 2013, 14, 1564-1572.
- (14) Seebach, D.; Overhand, M.; Kuhnle, F. N. M.; Martinoni, B.; Oberer, L.; Hommel, U.; Widmer, H. *Helvetica Chimica Acta* 1996, 79, 913-941.
- (15) Ahmed, S.; Beleid, R.; Sprules, T.; Kaur, K. *Org Lett* 2007, 9, 25-28.
- (16) Ahmed, S.; Kaur, K. *Chemical Biology & Drug Design* 2009, 73, 545-552.
- (17) Arvidsson, P. I.; Rueping, M.; Seebach, D. *Chemical Communications* 2001, 649-650.
- (18) Guarracino, D. A.; Chiang, H. J. R.; Banks, T. N.; Lear, J. D.; Hodsdon, M. E.; Schepartz, A. *Org Lett* 2006, 8, 807-810.
- (19) Hart, S. A.; Bahadoor, A. B. F.; Matthews, E. E.; Qiu, X. Y. J.; Schepartz, A. *J Am Chem Soc* 2003, 125, 4022-4023.
- (20) Vaz, E.; Dames, S. A.; Geyer, M.; Brunsveld, L. *Organic & Biomolecular Chemistry* 2012, 10, 1365-1373.
- (21) Vaz, E.; Pomerantz, W. C.; Geyer, M.; Gellman, S. H.; Brunsveld, L. *Chembiochem* 2008, 9, 2254-2259.
- (22) Kaur, K.; Sprules, T.; Soliman, W.; Beleid, R.; Ahmed, S. *Biochimica Et Biophysica Acta-Proteins and Proteomics* 2008, 1784, 658-665.
- (23) Fioroni, M.; Diaz, M. D.; Burger, K.; Berger, S. *J Am Chem Soc* 2002, 124, 7737-7744.
- (24) Roccatano, D.; Colombo, G.; Fioroni, M.; Mark, A. E. *Proc Natl Acad Sci U S A* 2002, 99, 12179-12184.
- (25) Sundaralingam, M.; Sekharudu, Y. C.; Yathindra, N.; Ravichandran, V. *Proteins-Structure Function and Genetics* 1987, 2, 64-71.

- (26) Mathews, J. L.; Gademann, K.; Jaun, B.; Seebach, D. J. Chem. Soc., Perkin Trans. 1 1998, 3331-3340.
- (27) Kritzer, J. A.; Tirado-Rives, J.; Hart, S. A.; Lear, J. D.; Jorgensen, W. L.; Schepartz, A. J Am Chem Soc 2005, 127, 167-178.
- (28) Raguse, T. L.; Lai, J. R.; Gellman, S. H. Helvetica Chimica Acta 2002, 85, 4154-4164.
- (29) Guntert, P. Methods Mol Biol 2004, 278, 353-378.
- (30) McMahon, B., Mays, D., Lipsky, J., Stewart, JA., Fauq, A., Richelson, E. Antisense Nucleic Acid Drug Dev. 2002, 12, 65-70.
- (31) Wuthrich, K. NMR of Proteins and Nucleic Acids, Wiley, New York 1986.

## FIGURE CAPTIONS

**Figure 1.** Structures of the  $\beta^3$ -peptides used in this study.  $\beta^3$ -Peptides **1**, **3-6** are derived from  $\beta^3$ -amido residues, and  $\beta^3$ -peptide **2** is synthesized from  $\beta^3$ -homo residues.

**Scheme 1.** General pathway of solid phase (top row) and solution phase (bottom row) syntheses of Fmoc- $\beta^3$ -amido-amino acids from Fmoc-L-Asp.

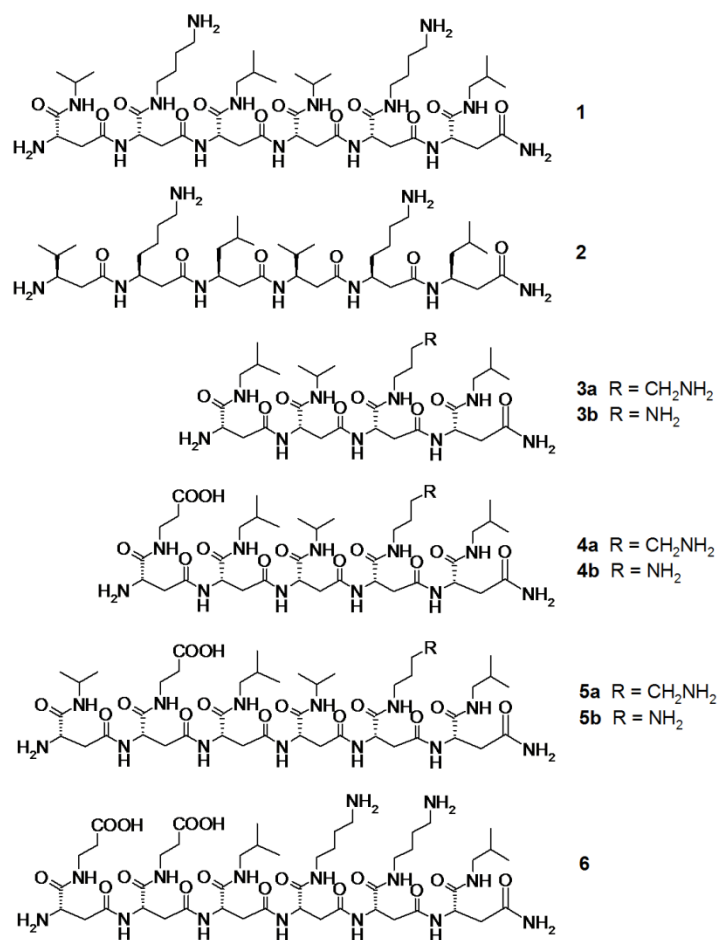
**Figure 2.** Circular dichroism (CD) spectra for  $\beta^3$ -hexapeptides (200  $\mu$ M) at 25 °C showing (a) **1**, **2**, **5a**, **5b**, and **6** in TFE, (b) **5a** in TFE, TFE/water, and aqueous solution, and (c) **6** in TFE, TFE/water, aqueous media, and PBC buffer (pH 7.4).

**Figure 3.** A comparison of the NOE of  $\beta^3$ -hexapeptides **1**, **2**, **5a** and **6** (in TFE) are summarized. \* denotes amide protons not observed due to exchange with solvent and X stands for H $\beta$  protons not observed due to overlap with solvent signal. Grey lines indicate ambiguous assignments.

**Figure 4.** 3D NMR solution structures of  $\beta^3$ -peptides **2** and **6** in TFE. The top view of the helices are shown using stick model (LHS) and overlay of 10 calculated structures (RHS) for **2** (a-b) and **6** (c-d).

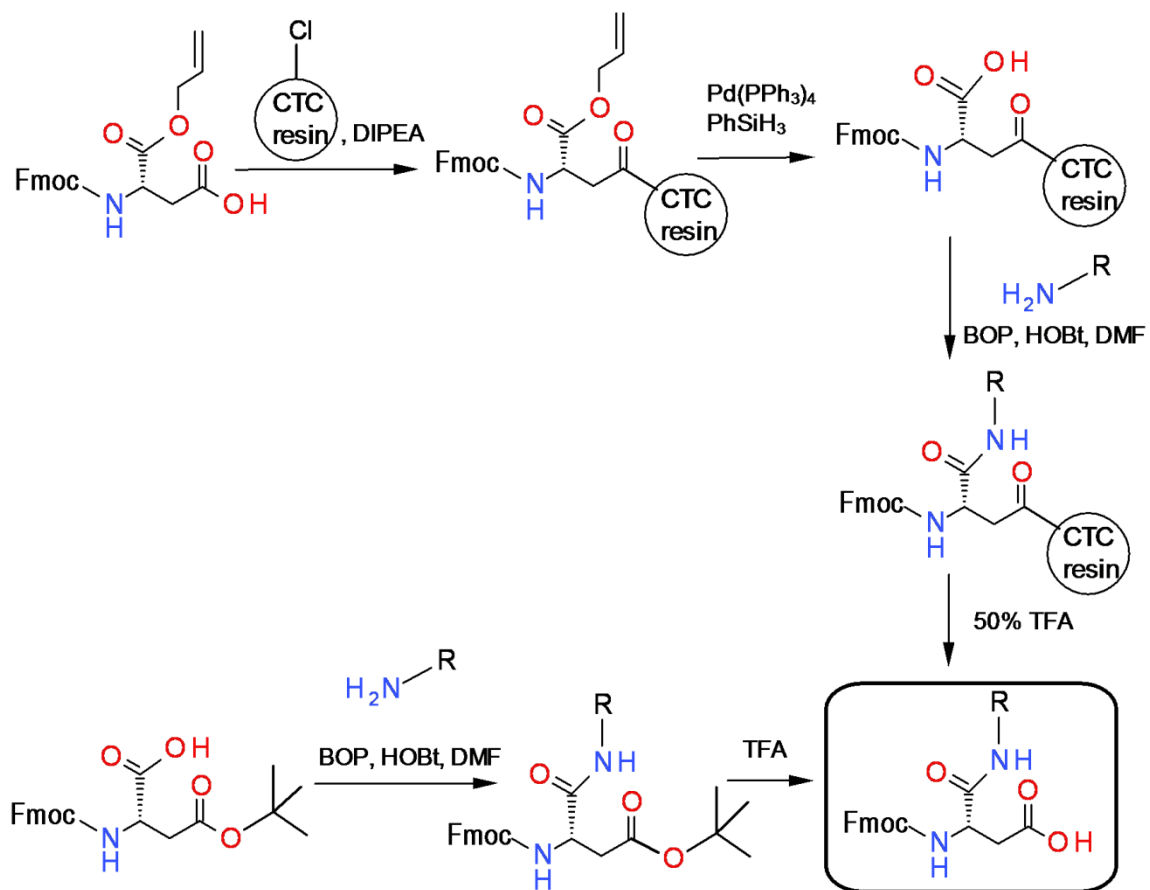
**Figure 5.** Solution conformation of  $\beta^3$ -hexapeptides **1** and **2** in TFE showing right-handed 14-helix for **1** and left-handed 14-helix for **2**.  $\beta^3$ -Peptide **1** has an additional amide group in each side chain.





**Figure 1.** Structures of the  $\beta^3$ -peptides used in this study.  $\beta^3$ -peptides **1**, **3-6** are derived from  $\beta^3$ -amido residues, and  $\beta^3$ -peptide **2** is synthesized from  $\beta^3$ -homo residues.

**Scheme 1.** General pathway of solid phase (top row) and solution phase (bottom row) syntheses of Fmoc- $\beta^3$ -amido-amino acids from Fmoc-L-Asp.



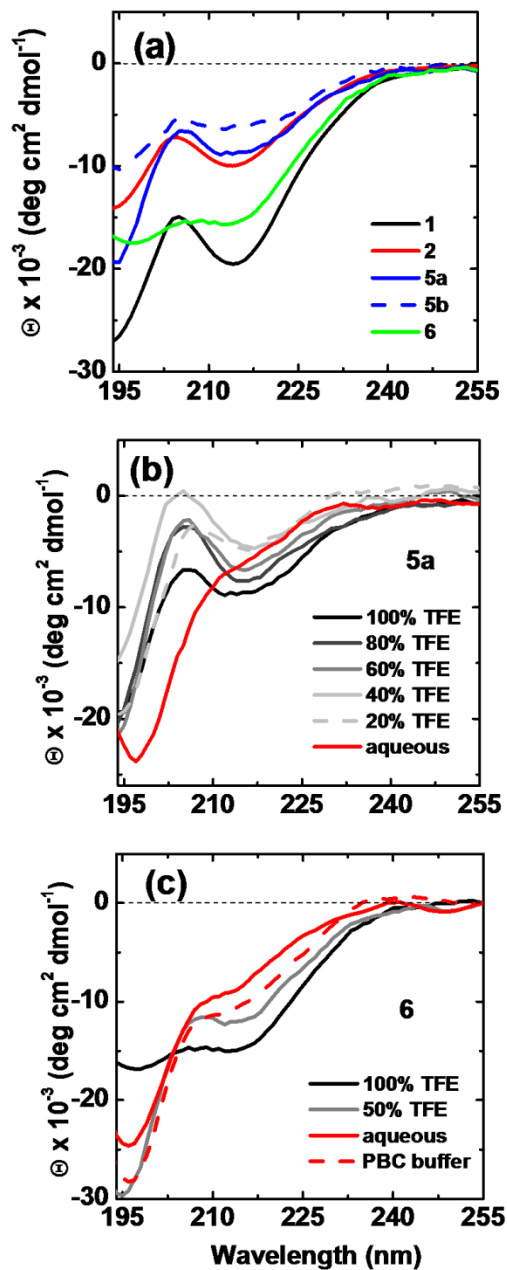


**Figure 2.** Circular dichroism (CD) spectra for  $\beta^3$ -hexapeptides (200  $\mu\text{M}$ ) at 25  $^\circ\text{C}$  showing (a) **1**, **2**, **5a**, **5b**, and **6** in TFE, (b) **5a** in TFE, TFE/water, and aqueous solution, and (c) **6** in TFE, TFE/water, aqueous media, and PBC buffer (pH 7.4).

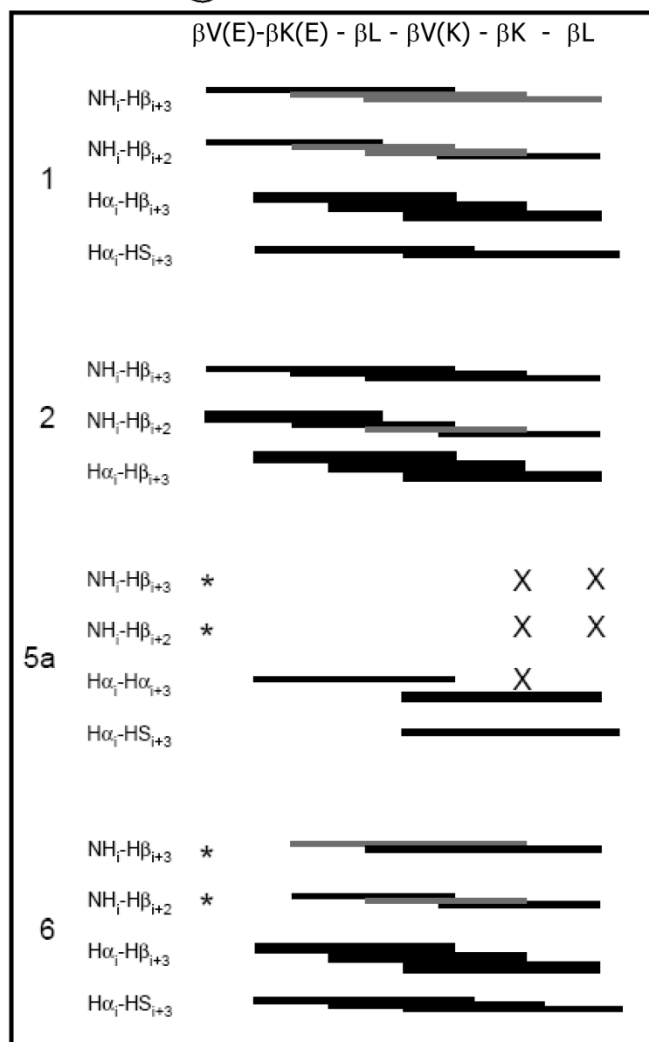
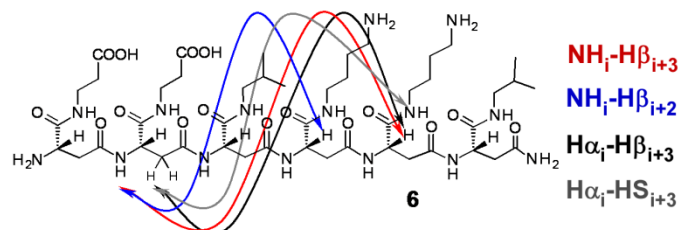


**Figure 3.** A comparison of the NOE of  $\beta^3$ -hexapeptides **1**, **2**, **5a** and **6** (in TFE) are summarized. \* denotes amide protons not observed due to exchange with solvent and X stands for  $H\beta$  protons not observed due to overlap with solvent signal. Grey lines indicate ambiguous assignments.

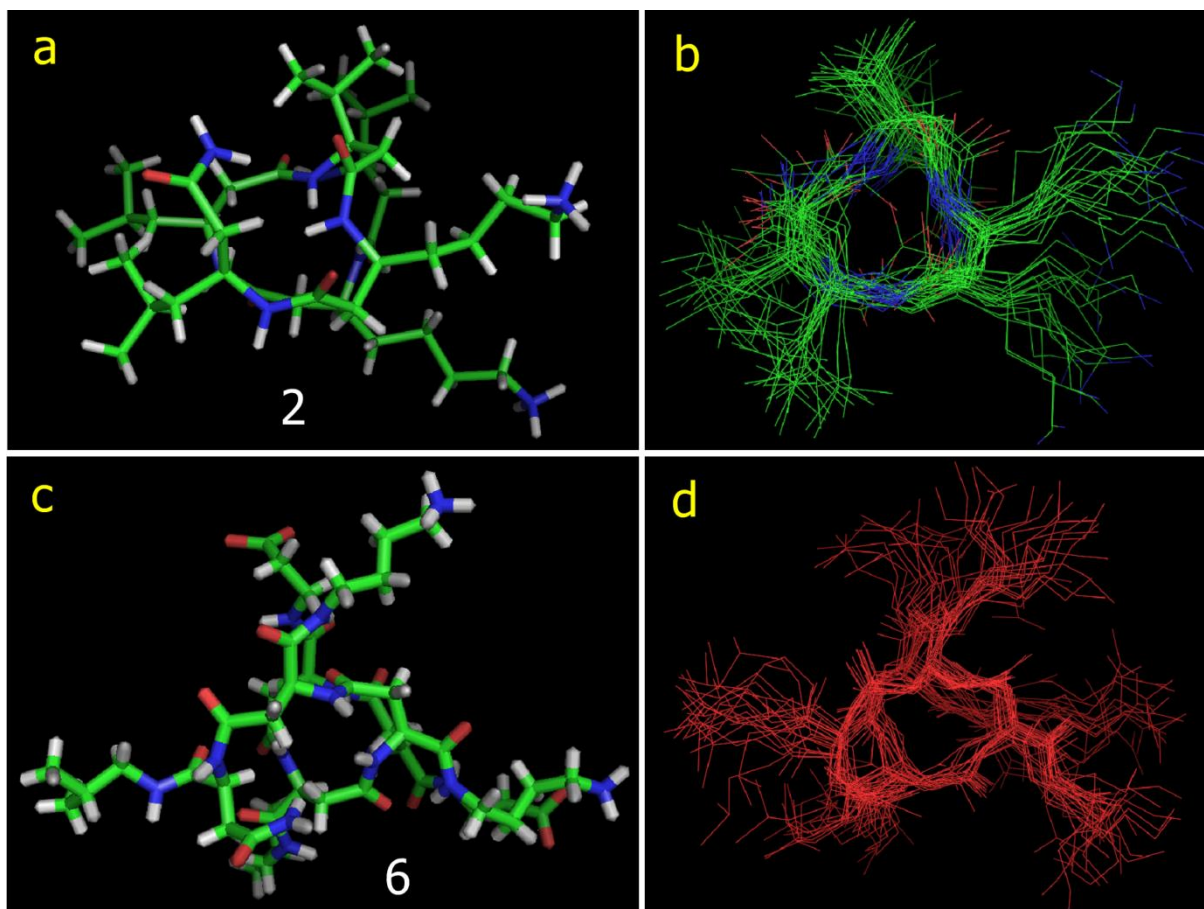


**Figure 4.** 3D NMR solution structures of  $\beta^3$ -peptides **2** and **6** in TFE. The top view of the helices are shown using stick model (LHS) and overlay of 10 calculated structures (RHS) for **2** (a-b) and **6** (c-d).

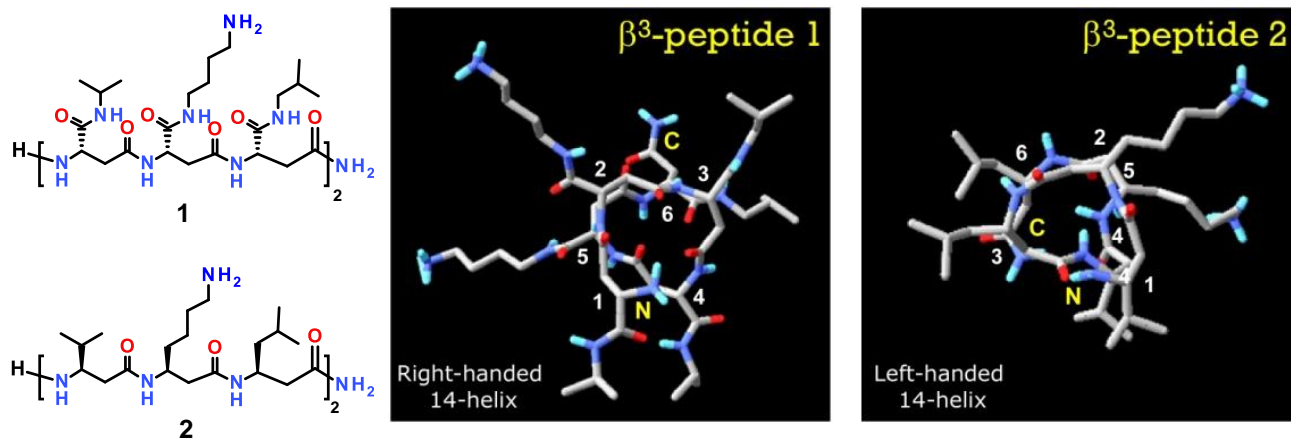


**Figure 5.** Solution conformation of  $\beta^3$ -hexapeptides **1** and **2** in TFE showing right-handed 14-helix for **1** and left-handed 14-helix for **2**.  $\beta^3$ -peptide **1** has an additional amide group in each side chain.